www.czasopisma.pan.pl PAN www.journals.pan.pl
POLSKA AKADEMIA NAUK

Arch. Metall. Mater. **69** (2024), 1, 151-156

DOI: https://doi.org/10.24425/amm.2024.147804

JI-A LEE[1], BONG-MIN JIN[1], JEONG-WHAN HAN[1*]

EVALUATION OF CLASSIFICATION POSSIBILITY OF COKE BREEZE BY DRAG FORCE

Sintered ore used as blast furnace burden materials is produced by mixing iron ore, coke, and limestone, then burning the coke and sintering the iron ore with the combustion heat. Among the coke charged, A particle size of 0.25 mm or less has an insignificant effect as a heat source and adhere to the surface of other materials to inhibit the reaction between oxygen and raw materials, thereby decreasing the quality of sintered ore. Therefore, to increase combustion efficiency, it is necessary to reduce the ratio of coke breeze in the charged coke.

In this study, theoretical calculation, experiment and simulation were conducted to investigate the possibility of size classification by drag force in the process of dropping coke after being transported through a belt conveyor. The height of belt conveyor was at 1m, and velocity of the belt was 1.5, 2.3, and 2.6 m/s, which were considered as experimental variables. After falling, the distribution of coke particle size according to the horizontal travel distance was confirmed, and a fall trajectory prediction formula model was created through the drag model of polydisperse system and compared with the experimental and analysis results.

Keywords: Powder processing; sintering process; coke breeze; numerical simulation; drag model

1. Introduction

To achieve global carbon neutrality, carbon reduction technologies are being demanded in all industries worldwide. Among domestic industries in South Korea, the iron·steelmaking process holds the highest proportion at 16.4% within the manufacturing industry [1], and it is characterized by carbon reduction-based processes. Therefore, the need for CO_2 reduction measures is urgent in the iron·steelmaking process. The steel industry is exploring the use of low-carbon technology and hydrogen as a reductant to meet its carbon neutrality objectives [2,3]. Research is being done into gas utilization techniques in the sintering process, such as exhaust gas capture and recycling, as a means of reducing CO_2 emissions [4-6]. However, coke breeze and anthracite, used as sintering binders, must be examined because they produce CO_2 during the sintering process. The effective particle size as a heat source for sintering binders ranges from 0.25 to 3.0 mm. The thermal efficiency is lower for coke breeze with a particle size of 0.25 mm or less because less heat is produced than for the effective-sized particle in sintering [7-9]. As a result, it is advantageous to reduce CO_2 emissions when the effective-sized particle fraction of the coke charged into the sintering process increases because it allows for a reduced binder input for a given heat quantity. Additionally, the fine particles in coke breeze significantly impacts the quality of sintered ore because it creates an adhesive layer on the surface of other raw materials that prevents sintering [10,11]. One easily applicable method for separating materials based on particle size in industrial settings is sieving and classification. Sieving offers the advantage of excellent separation efficiency and low equipment cost, but it faces the issue of reduced separation efficiency and high maintenance costs as the sieve aperture size decreases. On the other hand, classification allows for effective separation of materials with high adhesion properties and requires minimal maintenance. However, the initial equipment cost is a significant drawback [12,13]. In the sintering process, coke, which is used as a binding agent, requires the separation of fine particles below 250 μm. Additionally, considering that a conveyor belt for transporting sintering materials is already installed, the classification method is deemed more suitable as it eliminates the need for additional equipment.

This study aimed to determine whether it was possible to classify small-sized particle by drag force while falling after coke was transported along a belt conveyor for raw material transportation during the sintering process. The impact of particle size on fall behavior was compared and examined through theoretical

[1] INHA UNIVERSITY, DEPARTMENT OF MATERIALS SCIENCE AND ENGINEERING, 100 INHA-RO, MICHUHOL-GU, INCHEON 22212, REPUBLIC OF KOREA

* Corresponding author: jwhan@inha.ac.kr

© 2024. The Author(s). This is an open-access article distributed under the terms of the Creative Commons Attribution-NonCommercial License (CC BY-NC 4.0, https://creativecommons.org/licenses/by-nc/4.0/deed.en which permits the use, redistribution of the material in any medium or format, transforming and building upon the material, provided that the article is properly cited, the use is noncommercial, and no modifications or adaptations are made.

calculations and experiments. Additionally, a simulation of falling coke was run under identical conditions to the experiment to investigate the particle size distribution according to the horizontal positions and properly assess the classification possibility.

2. Experiment

2.1. Calculation of fall trajectory

According to Williams et al. [14], there is a particle size-based segregation mechanism, and a flying particle's horizontal travel distance causes difference in proportion to the square of the particle size [15]. The trajectory can be determined by calculating the travel distance in the horizontal and vertical directions using the equations below, respectively, to compare the fall trajectories according to the particle sizes on the belt conveyor:

Horizontal travel distance,

$$s_1 = s_0 + V_0\left(t_1 - t_0\right) - \frac{1}{2}a_0\left(t_1 - t_0\right)^2 \tag{1}$$

Vertical travel distance,

$$h = H - \frac{1}{2}gt^2 \tag{2}$$

Where, s, V, t, a, h, H, and g stand for the horizontal travel distance, velocity, time, deceleration, vertical travel distance, initial particle height, and gravitational acceleration. The subscripts 0 and 1 represent the previous and current calculation steps. Deceleration a was applied in the horizontal direction by determining the drag coefficient based on the particle size. The Beetstra model proposed to calculate the drag force for a random arrangement containing particles of varied sizes can be used to calculate the polydisperse system [16]. The vertical travel distance was determined using the gravitational acceleration.

2.2. Falling coke experiment

Fig. 1(a) shows a belt conveyor system for a coke breeze classification experiment. Experiments were run for comparison with the theoretically predicted trajectories. The hopper opener was opened to start the experiment after loading coke into the charging hopper and running the belt conveyor. Coke was loaded at a rate of 0.3 kg/s throughout the experiment, and the belt conveyor's speed was set at 1.5, 2.3, and 2.6 m/s.

2.3. Simulation of DEM-CFD coupling

The discrete element method is a numerical analysis of powder that calculates the motion of particles with a mass while tracking the motion of all particles [17]. In this situation, it is calculated by applying the governing equation below to divide the motion into translational and rotational motion [18].

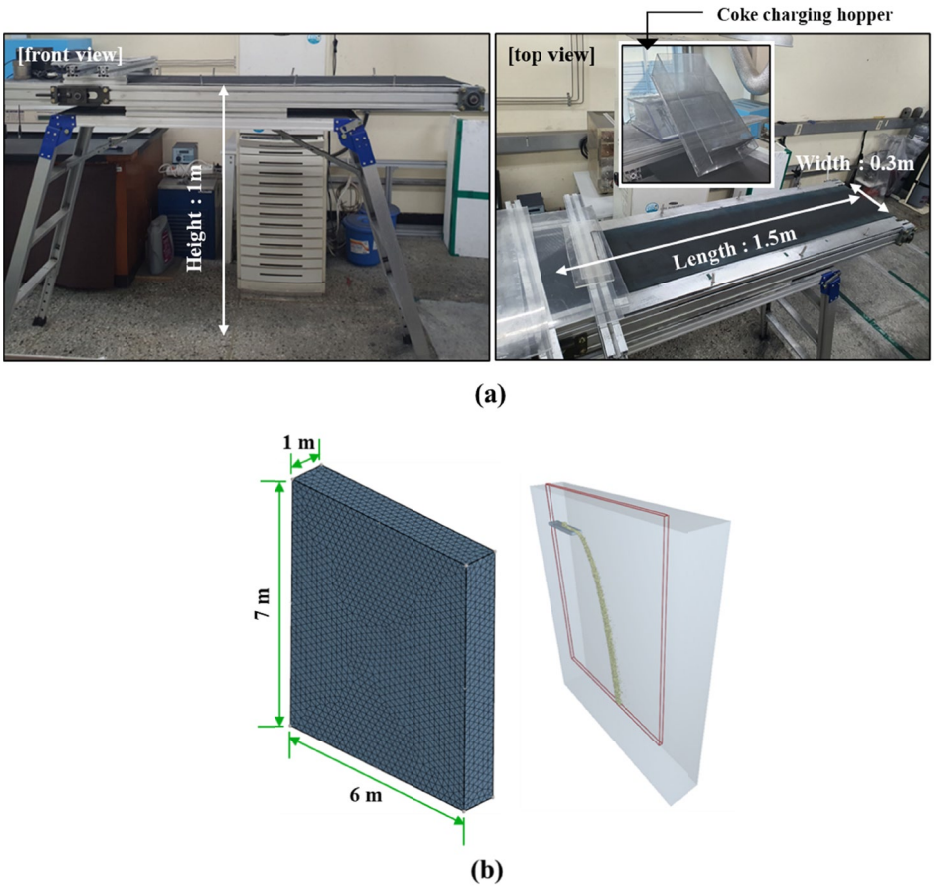

Fig. 1. (a) Belt conveyor equipment, (b) Computational domain for simulation

$$m_p \frac{dv_p}{dt} = \sum_{j \neq i}^{N_c} F_c + F_f + F_g \tag{3}$$

$$I_p \frac{d\omega_p}{dt} = R_p \sum_{j \neq i}^{N_c} \left(F_{cs} - F_r \right) \tag{4}$$

Where, m_p, v_p, t, F_c, N_c, F_f, F_g, I_p, ω_p, R_p, F_{cs}, F_r stand for the particle mass, particle velocity, time, contact force between the particles, number of particles in contact, fluid force acting on the particles, gravity, moment of inertia, angular velocity, particle radius, tangential force in the shear direction, and rolling resistance.

In computational fluid dynamics, fluid phenomena are calculated using algorithms for numerical techniques. The Navier-Stokes equation is used in this situation as the governing equation, and the conservation equations for mass, momentum, and energy are as follows: [19]

$$\frac{\partial \rho}{\partial t} + \nabla \cdot \left(\rho \vec{u} \right) = 0 \tag{5}$$

$$\rho \frac{\partial \vec{u}}{\partial t} + \left(\rho \vec{u} \cdot \nabla \right) \vec{u} = -\nabla p + \rho b + \nabla \cdot \tau \tag{6}$$

$$\frac{\partial \left(\rho E \right)}{\partial t} + \nabla \cdot \left(\rho E \vec{u} \right) = \nabla \cdot \left(k \nabla T \right) - \nabla \cdot \left(p \vec{u} \right) + \\ + \vec{u} \cdot \left(\nabla \cdot \tau \right) + \nabla \vec{u} : \tau + \rho b \cdot \vec{u} + S \tag{7}$$

Where, ρ, t, $\vec{u}$, p, b, τ, E, $k\nabla T$, S refer to the fluid density, time, flow velocity vector, pressure, gravity, viscous stress tensor, total energy, heat flux according to Fourier's Law, and heat source.

The analysis geometry is shown in Fig. 1(b) and the whole domain was set wide enough that the wall wouldn't affect the flow. The coupling model is two-way coupling (Bi-directional coupling) utilized when particles influence the flow. This is a model that allows DEM and CFD to run simultaneously, enabling continuous data exchange. The flow is set to laminar conditions based on the Beetstra drag model. The analysis conditions were the same as the experiment, with speed changes of 1.5, 2.3, and 2.6 m/s were used; the boundary conditions of the simulation were modeled identically to the experimental conditions, and the detailed values are shown in TABLE 1.

3. Results and discussion

3.1. Fall trajectory prediction

Fig. 2(a) and (b) show the fall trajectories derived from theoretical calculations and experiments with conveyor speeds of 1.5 to 2.3 and 2.6 m/s. At 1.5 m/s, it falls with the shortest horizontal travel distance and the narrowest track width. At the fastest speed of 2.6 m/s, the horizontal travel distance is the longest, and the width of the trajectory is the widest. Both theoretical

TABLE 1

Condition of simulation

		Experiment condition		Simulation condition		
Particle size	Diameter of particle	Sieve 1	5.0~	large	3.0	[mm]
		Sieve 2	2.8~5.0			
		Sieve 3	2.0~2.8	medium 1	1.5	
		Sieve 4	1.0~2.0			
		Sieve 5	0.5~1.0	medium 2	0.75	
		Sieve 6	0.25~0.5			
		Sieve 7	~0.25	small	0.25	
	Charging ratio	Sieve 1	9	large	28.48	[%]
		Sieve 2	20			
		Sieve 3	8	medium 1	23.16	
		Sieve 4	15			
		Sieve 5	12	medium 2	22.87	
		Sieve 6	11			
		Sieve 7	25	small	25.49	
Modeling of particle	Shear modulus				1	[MPa]
	Poisson's ratio				0.25	[-]
	Density of particle				1000	[kg/m^3]
	Coefficient of static friction		particle-particle		0.664	[-]
			particle-wall		0.45	
	Coefficient of restitution		particle-particle		0.18	[-]
			particle-wall		0.15	
	Coefficient of rolling friction		particle-particle		0.764	[-]
			particle-wall		0.7	
Analysis condition	Charging speed				0.3	[kg/s]
	Drag model				Beetstra model	
	Scale factor				5.0	

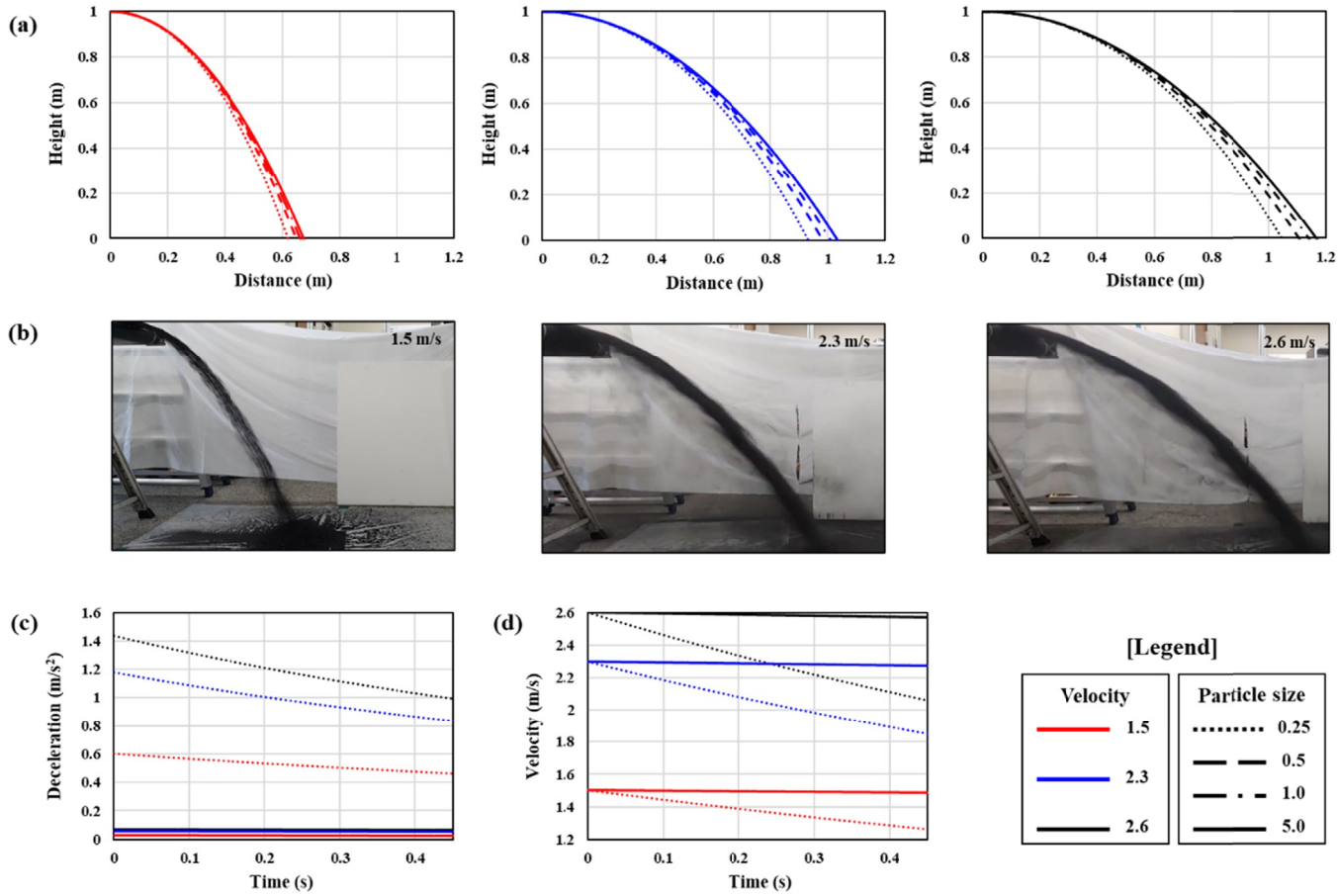

Fig. 2. Fall behaviors in theoretical calculation and experiment by velocity (a) Fall trajectory by theoretical calculation (b) Fall trajectory by experiment (c) change of deceleration (d) change of particle velocity

calculations and experimental findings yield the same result. The deceleration effect is expected to be related to the varying horizontal travel distance depending on the particle size. According to Newton's second law, deceleration is proportionate to drag and inversely proportionate to mass. In this case, the drag force is proportionate to the cutting area of the particle and the square of the speed, and the mass is proportionate to the volume of the particle. Therefore, the area term is offset. The deceleration is, therefore, inversely related to particle size. Through this, it can be observed that small-sized particles experience excessive deceleration compared to effective and large-sized particles, resulting in a difference in falling distance. This indicates the feasibility of classifying small-sized particles. Additionally, when the initial velocity increases, the trajectory width tends to increase. In Fig. 2(c) and (d), showing the change in deceleration and particle velocity over time for particles of 0.25 mm and 5.0 mm per speed condition, it can be confirmed that the negative slope values increase for both the deceleration and velocity of the small-sized particles as the conveyor speed increases. This implies that both acceleration and velocity decrease over time. Equation (1) confirms that the trajectory width expands as the conveyor speed increases, as the horizontal travel distance is more influenced by the velocity than the deceleration. As the conveyor speed rises, it is anticipated that classification will become easier.

3.2. Classification efficiency analysis

The simulation was conducted, and Fig. 3 shows the falling behavior with velocity. It was confirmed that, as the speed increases, the trajectory width and horizontal travel distance increase. In practical processes, dampers may be attached to facilitate classification or segregation. The classification damper plays a role in dividing the falling path of transported materials into inner and outer spaces, typically taking the form of a plate with a linear or curved shape. Additionally, since the particle size distribution of the overall processed materials is constantly changing, it is necessary to introduces a rotational feature that allows for easy angle adjustment based on operational conditions. Numerous studies exist that examine the minimization of the difference between the average size of separated particles and the target average size through such processing equipment [20]. Therefore, by attaching a damper, it will be possible to classify the coke into the inside and outside areas based on damper position, as indicated in Fig. 4(a). The classification efficiency aims to classify small-sized particles into the inside area and effective-sized particles into the outside area. Although the potential classification is anticipated as the velocity increases, it is difficult to precisely manage the position of the damper in real operations, and abrasion due to the fall of the raw material also exists. Therefore, as shown in Fig. 4(a), the optimal clas-

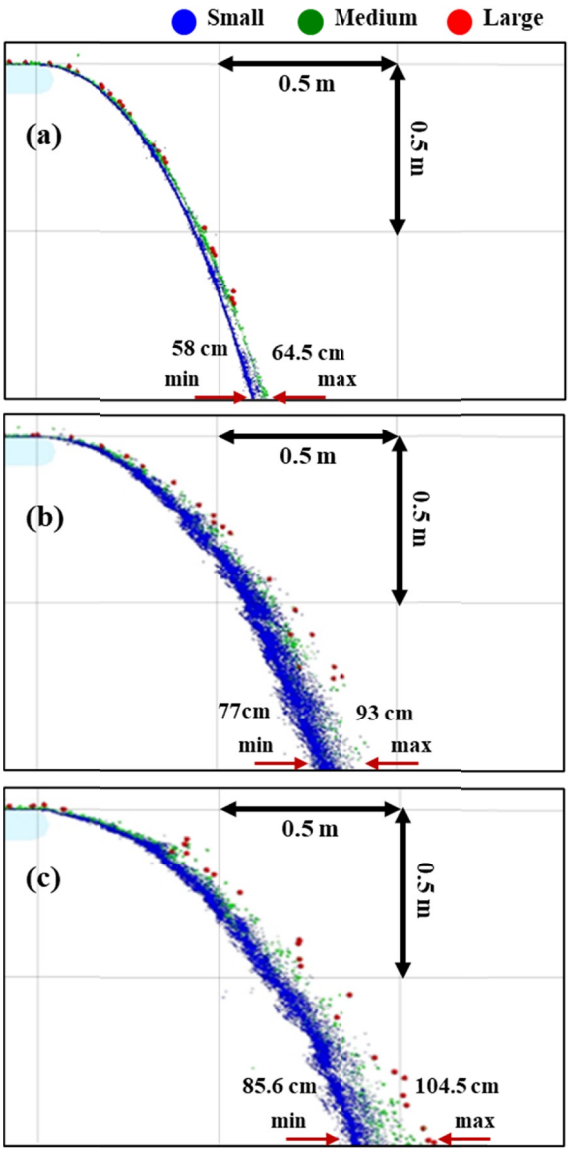

Fig. 3. Falling behavior by velocity (a) 1.5 m/s, (b) 2.3 m/s and (c) 2.6 m/s

sification position (OCP) for each condition was determined, and the particle size distribution was compared at 5 positions moved 2 cm and 4 cm left and right from the OCP, respectively. At 1.5 m/s, –2 and OCP, it shows good classification; however, in the case of +2, the ratio of effective-sized particle in the in increases rapidly, and in the cases of –4 and +4, all raw materials escape from one side only. At 2.3 m/s, the differential separation is better the more they move in the + direction compared to OCP, but effective-sized particles are also distributed more. It is thought to be because the overlapping ranges of the different particle size has been expanded. Finally, the ideal data was obtained at 2.6 m/s, and the classification of small-sized particles was accomplished in all points ranging from –4 to +4. Therefore, moving the damper up to a margin of error ±4 cm is conceivable, and good classification control is believed to be achievable. However, using a damper necessitates extra research into fundamental properties and characteristics of the material of the damper.

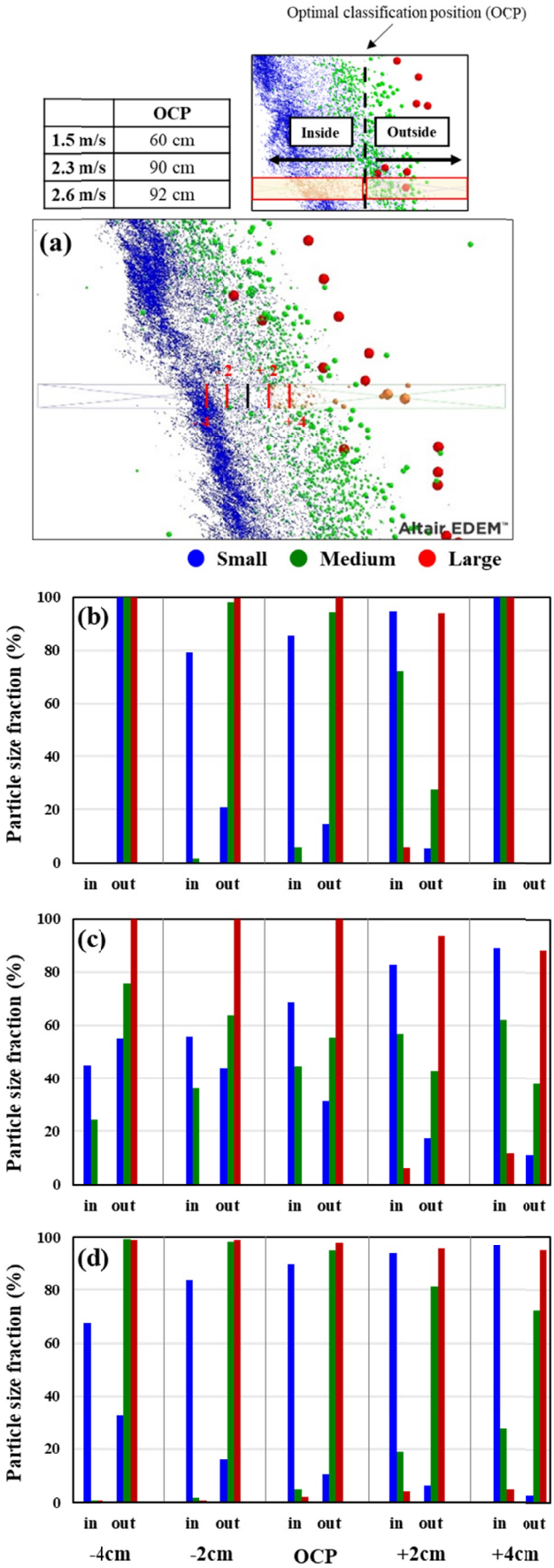

Fig. 4. Changes in particle size distribution by classification position (a) method of classification position setting, (b) change in particle size distribution in 1.5 m/s, (c) change in particle size distribution in 2.3 m/s, (d) change in particle size distribution in 2.6 m/s

4. Conclusions

In this study, theoretical calculations, experiments, and simulations were conducted to evaluate the possibility of powder classification by orbital segregation during the raw material transfer process for the purpose of classifying raw materials of small-sized particle that do not belong to the effective particle size range for coke, which is input as a sinter binder.

As the conveyor belt's speed increases, the horizontal travel distance increases, and the width of the trajectory widens. This is because as the speed increases, the rate of decrease for both the deceleration and particle velocity increase for each particle size, but the horizontal travel distance is more affected by the particle velocity than the deceleration. The same trend was confirmed in theoretical calculations, experiments, and simulations.

The best position for damper attachment has been determined, and if the damper is slightly displaced at a slower speed, classification does not occur at all. Under conditions of 2.6 m/s, the classification of coke breeze was confirmed to be possible, even if an error of ±4 cm based on the OCP occurred. Additional study is required into the impacts of damper specifications such as length, angle, as well as physical properties of material to apply these findings to actual process.

Finally, it was confirmed that small-sized particles with lower thermal efficiency than the effective-sized particles can be easily classified during the raw material transportation process. As a result, particles larger than the effective-sized particles in the sintering process can be directed to subsequent processes for use as a heat source for iron ore sintering. The separated small-sized particles can undergo an agglomeration process to improve their particle size before being reintroduced, leading to increased energy efficiency and reduced CO_2 emissions.

REFERENCES

[1] Greenhouse Gas Inventory and Research Center, Greenhouse Gas Emissions in 2020, www.2050cnc.go.kr/flexer/view/BOARD_ATTACH?storageNo1284 (2022).
[2] F. Patisson, O. Mirgaux, Metals **10**, 922 (2020).
[3] S.H. Yi, W.J. Lee, Y.S. Lee, W.H. Kim, J. of the Korean Inst. of Met. & Mater. **59**, 41 (2021).
[4] H. Zhang, M. Rao, Z. Fan, Y. Zhang, G. Li, T. Jiang, ISIJ Int. **52**, 2139 (2012).
[5] D. Zhu, Y. Xue, J. Pan, C. Yang, Z. Guo, H. Tian, X. Wang, Q. Huang, L. Pan, X. Huang, Powder Technol. **373**, 727 (2020).
[6] X. Fan, G. Wong, M. Gan, X. Chen, Z. Yu, Z. Ji, J. Clean. Prod. **235**, 1549 (2019).
[7] N. Tahanpesaranedezfuly, A.H. Moghadam, TMS 2012 141st Annual Meeting and Exhibition. Supplemental Proceedings. **1** (2012).
[8] D.F. Gonzalez, I.R. Bustinza, J. Mochon, C.G. Gasca, L.F. Verdeja, JOM-J. Min. Met. Mat. S. **68**, 2089 (2016).
[9] Z. Cheng, J. Yang, L. Zhou, Y. Liu, Z. Guo, Q. Wang, Energy Conversion and Management **125**, 254 (2016).
[10] T. Umadevi, A.V. Deodhar, S. Kumar, C.S.G. Prasad, M. Ranjan, Ironmak. Steelmak. **35**, 567 (2008).
[11] L. Xiong, Z. Peng, F. Gu, L. Ye, L. Wang, M. Rao, Y. Zhang, G. Li, T. Jiang, Power Technol. **340**, 131 (2018).
[12] Korean patent No.10-1023111, March 10 (2011).
[13] Korean patent No.10-2020-0122895, October 28 (2020).
[14] J.C. Williams, Powder Technol. **15**, 245 (1976).
[15] K.M. Kim, J.H. Kim, J.H. Kwon, J.A. Lee, J.W. Han, Arh. Metall. Mater. **64**, 495 (2019)
[16] R. Beetstra, M.A. van der Hoef, J.A.M. Kuipers, AIChE J. **53**, 489 (2007).
[17] J.H. Jeong, J.I. Choi, J. Korean powder Metall. Inst. **28**, 1 (2021)
[18] S. Ueda, T. Kon, H. Kurosawa, S. Natsui, T. Ariwama, H. Nogami, ISIJ Int. **55**, 1232 (2015).
[19] Altair, Altair AcuSolve Training Manual (2021).
[20] Korea Institute of Geoscience and Mineral Resources, TRKO201200005157, scienceon.kisti.re.kr/commons/util/originalView.do?cn=TRKO201200005157&dbt=TRKO&rn= (2005).